Carbohydrate Polymers 101 (2014) 203–212

Contents lists available at ScienceDirect

Carbohydrate Polymers

journal homepage: www.elsevier.com/locate/carbpol

Relationship between structure and cytocompatibility of divinyl sulfone cross-linked hyaluronic acid

Jui-Yang Lai [a,b,c,*]

[a] Institute of Biochemical and Biomedical Engineering, Chang Gung University, Taoyuan 33302, Taiwan, ROC
[b] Biomedical Engineering Research Center, Chang Gung University, Taoyuan 33302, Taiwan, ROC
[c] Molecular Medicine Research Center, Chang Gung University, Taoyuan 33302, Taiwan, ROC

ARTICLE INFO

Article history:
Received 20 July 2013
Received in revised form
17 September 2013
Accepted 18 September 2013
Available online 25 September 2013

Keywords:
Hyaluronic acid
Divinyl sulfone
Cross-linker concentration
Molecular structure
Cytocompatibility
Retinal pigment epithelium

ABSTRACT

Hyaluronic acid (HA), a carbohydrate polymer naturally found in the eye, has been chemically modified by cross-linking to enhance its performance as a drug carrier. Although the treatment of HA with divinyl sulfone (DVS) is reported, the effects of cross-linker concentration on the biomaterial-mediated retinal pigment epithelial (RPE) cellular responses are yet to be investigated. This paper explores, for the first time, the relationship between molecular structure and cytocompatibility of HA hydrogels cross-linked with DVS of varying concentrations (0–100 mM). The results showed that with increasing DVS concentration, the sulfur content and sulfonyl-bis-ethyl cross-link amount are increased and the mechanical stability and resistance against enzymatic degradation are enhanced, indicating the crucial role of cross-linker in the alteration of structure and property of this polysaccharide biomaterial. The cell viability, pro-inflammatory gene and cytokine expression, and glutamate uptake were suggested to be indicative of cytocompatibility and found to be strongly dependent on the cross-linker concentration.

1. Introduction

Hyaluronic acid (HA) is a naturally occurring linear anionic polysaccharide found in aqueous and vitreous humor of the eye, synovial fluid of the joints and connective tissues such as skin, arterial wall, umbilical cord and rooster comb (Hahn, Jelacic, Maier, Stayton, & Hoffman, 2004). It is comprised of repeating disaccharide units of D-glucuronic acid and *N*-acetyl-D-glucosamine. In clinical ophthalmology, HA has been extensively used as an artificial tear ingredient for dry eye treatment (McDonald, Kaye, Figueiredo, Macintosh, & Lockett, 2002) and a viscoelastic agent for cataract surgery (Jeng, Hoyt, & McLeod, 2004). Therefore, HA is regarded as one of the most important ophthalmic biomaterials. Our group has previously reported that carbodiimide cross-linked HA hydrogel discs can be applied to overcome the fragility of thermally detached corneal endothelial cell sheets during surgical manipulation (Lu, Lai, Ma, & Hsiue, 2008). The HA-based delivery system may have potential to establish a minimally invasive technique for intraocular grafting of bioengineered corneal endothelium, which is critical to achieve better restoration outcomes. More recently, HA-coated tissue culture plates have been fabricated to control the formation of corneal stromal cell spheroids during keratocyte growth (Lai & Tu, 2012). For applications as therapeutic transplants in corneal ulcer, the multicellular spheroids are featured with enhanced cell phenotype and biosynthetic capacity.

Age-related macular degeneration is a sight-threatening disease that affects the posterior segment of the eye and leads to reduced visual acuity. Pharmacological therapy by intravitreal instillation of a suitable drug is considered to be a possible way to inhibit further choroidal neovascularization (Fine, Berger, Maguire, & Ho, 2000). Although this administration route is effective to avoid adverse effects caused by systemic administration, it is highly desired to design a drug carrier that provides a sustained-release formulation and achieves a high drug concentration at the site of action. In terms of biomaterials selection for carrier systems, HA is preferred because of its essential role in regulating the hyaluronan synthase/hyaluronan/CD44 signaling system in the posterior eye segment and maintaining the functional structure of retina and choroid (Murata & Horiuchi, 2005). However, HA is known to have an extremely high capacity for water absorption, thereby exhibiting rapid dissolution in aqueous environments. As reported in the literature, a short residence time of HA molecule in tissue (only a few days (Zhao, 2006)) greatly restricts its biomedical applications. To overcome this drawback, we have devised a method of modifying polysaccharide biomaterials to improve the hydrolytic stability of HA (Lu et al., 2008). 1-Ethyl-3-(3-dimethyl aminopropyl)

* Correspondence to: Institute of Biochemical and Biomedical Engineering, Chang Gung University, Taoyuan 33302, Taiwan, ROC. Tel.: +886 3 211 8800x3598; fax: +886 3 211 8668.
E-mail address: jylai@mail.cgu.edu.tw

0144-8617/$ – see front matter © 2013 Elsevier Ltd. All rights reserved.
http://dx.doi.org/10.1016/j.carbpol.2013.09.060

carbodiimide is a zero-length cross-linker that can induce ester bond formation between the hydroxyl and carboxyl groups of HA. Following the cross-linking treatment, the HA molecules join together without added bridging moieties. In contrast, glutaraldehyde, a non zero-length cross-linker, is incorporated in the cross-linked HA materials. A more rigid biopolymer network structure is constructed since the cross-linking agent participates in the formation of covalent bonds.

Glutaraldehyde, despite having a better cross-linking performance as compared with carbodiimide, poses a noticeable problem in cytotoxicity. The specific linkages (i.e., Michael-type adducts with terminal aldehydes) present in the cross-linking structure possibly cause apoptosis and harmful irritation to cultured retinal pigment epithelial (RPE) cells (Lai, Li, & Wang, 2010). Divinyl sulfone (DVS) is another non zero-length cross-linker and has been widely used to chemically modify HA materials for the prevention of postsurgical soft tissue adhesion (Sannino et al., 2004), stimulation of functional endothelialization (Oh et al., 2008), and tissue augmentation (Ibrahim, Kang, & Ramamurthi, 2010). In light of these promising reports, our attention is turned to evaluate the potential of DVS cross-linked HA for ophthalmic use. Given that the chemical cross-linking may be detrimental to the biocompatibility of the carbohydrate polymers, it is first necessary to examine the safety of HA materials treated by DVS. Here, we aimed to perform an in vitro test to explore the RPE cellular responses to DVS cross-linked HA hydrogels. After modification with varying concentrations of DVS, the HA sheets were characterized by energy dispersive X-ray spectroscopy (EDS) to monitor the level of incorporated DVS in the biopolymer. Subsequently, the Fourier transform infrared spectroscopy (FTIR) was used to investigate molecular interactions in cross-linked samples. Stability improvement was determined by mechanical and degradation tests. In order to give insight into the role of cross-linker concentration on cell viability and pro-inflammatory gene and cytokine expressions, the ARPE-19 cultures exposed to chemically modified carbohydrate polymers were analyzed by Live/Dead fluorescent labeling and quantitative real-time reverse transcription polymerase chain reaction and enzyme-linked immunosorbent assay. Additionally, the glutamate uptake was measured to evaluate the function of cultured RPE cells in the presence of polysaccharide biomaterials. This study explored for the first time the relationship between molecular structure and cytocompatibility of DVS cross-linked HA. The obtained information from ocular cell-carbohydrate polymer interactions will facilitate further development of cell/drug carriers for potential ophthalmic applications.

2. Materials and methods

2.1. Materials

Hyaluronic acid sodium salt was obtained from Kewpie (Tokyo, Japan) as a dry powder. It was made by fermentation method and was highly purified. According to information from the supplier, the HA samples used in this study had a weight-average molecular weight of around 1100 kDa. Divinyl sulfone (DVS) supplied from Tokyo Chemical Industry (Tokyo, Japan) was purified by distillation under reduced pressure prior to use. Hyaluronidase type V from sheep testes (1770 units/mg) and bovine serum albumin (BSA) were purchased from Sigma–Aldrich (St. Louis, MO, USA). Deionized water used was purified with a Milli-Q system (Millipore, Bedford, MA, USA). Balanced salt solution (BSS, pH 7.4) was obtained from Alcon Laboratories (Fort Worth, TX, USA). Phosphate-buffered saline (PBS, pH 7.4) was acquired from Biochrom AG (Berlin, Germany). Dulbecco's modified Eagle's medium/Ham's F12 nutrient mixture (DMEM/F12) and TRIzol reagent were purchased from Gibco-BRL (Grand Island, NY, USA). Fetal bovine serum (FBS) and the antibiotic/antimycotic (A/A) solution (10,000 U/ml penicillin, 10 mg/ml streptomycin and 25 μg/ml amphotericin B) were obtained from Biological Industries (Kibbutz Beit Haemek, Israel). Radioactive [^{3}H]glutamate was purchased from Amersham (Little Chalfont, UK). All the other chemicals were of reagent grade and used as received without further purification.

2.2. Cross-linking of HA sheets by DVS

The HA hydrogel samples were prepared by solution casting methods. An aqueous solution of 0.5 wt% HA was poured into a polystyrene planar mold (5 cm^2 × 5 cm^2, 1.5 cm depth), and air-dried for 3 days at 25 °C to obtain hydrogel sheets (approximately 700 μm in thickness). The HA hydrogels (100 mg) were further treated with DVS according to the protocols used for fabrication of chemically cross-linked HA molecules (Lai, Ma, et al., 2010; Lu et al., 2008). The samples were cross-linked by directly immersing the hydrogel sheets in an alkaline water solution (0.02 N NaOH, pH = 12) containing DVS of varying concentrations (25–100 mM). The cross-linking reaction was allowed to proceed at 25 °C for 24 h. In order to remove unreacted components and neutralize the pH, the resulting samples were thoroughly washed with deionized water and then exhaustively dialyzed (MWCO 3500, Spectra/Por® Dialysis Membrane, Rancho Dominguez, CA, USA) for 24 h against deionized water. The cross-linked HA materials were dried in vacuo for 2 days. In this study, the HA hydrogels modified with cross-linker concentrations of 25, 50, and 100 mM were designated as HA-DVS025, HA-DVS050, and HA-DVS100, respectively. HA sheets without chemical cross-linking (designated as HA-DVS000) were used for comparison.

2.3. Characterization of DVS cross-linked HA sheets

The samples were analyzed with an energy dispersive X-ray spectroscope (Oxford Instruments, Concord, MA, USA) according to a previously published method (Lai, Chen, Hsu, Lee, & Lin, 2005). Small pieces of the sheets were cut off and mounted onto stubs using double-sided adhesive tape. The elemental distribution was determined using X-ray elemental mapping. Data acquisition was performed with an accelerating voltage of 10 kV. Results were averaged on three independent runs.

The Fourier transform infrared spectroscopy of various samples was performed using a FT-730 ATR-FTIR Spectrophotometer (Horiba, Kyoto, Japan) (Lai & Hsieh, 2012). The spectra were recorded between 3700 and 700 cm^{-1}, with a resolution of 8 cm^{-1}. The data were analyzed using FTIR spectrum software (Horiba) to obtain quantitative peak information. The results were the average of three independent experiments. In this study, the FTIR spectra from the DVS groups were obtained by measuring DVS liquid samples (Ellzy, Jensen, & Kay, 2003).

2.4. Mechanical tests

In the tensile tests, the cross-linked HA sheets were placed in an environment with humidity of 75% for 24 h (Lai et al., 2009). Then, the dumbbell-shaped samples were prepared by cutting wet membranes under pressure with a suitable mold. The gauge length of the specimens was 10 mm and the width was 5 mm. Sample thicknesses were measured at three different points with a Pocket Leptoskop electronic thickness gauge (Karl Deutsch, Germany) and the average was taken. The stress at break and Young's modulus values of HA samples were determined using an Instron Mini 44 universal testing machine (Canton, MA, USA). All measurements

were performed at 25 °C and a relative humidity of 50% using a crosshead speed of 0.5 mm/min. Results were averaged on eight independent runs.

2.5. In vitro degradation tests

To measure the extent of degradation, each HA sheet was first dried to constant weight (W_i) in vacuo. The test samples were immersed in BSS containing 400 units/ml hyaluronidase and incubated at 37 °C with reciprocal shaking (50 rpm) in a thermostatically controlled water bath. At specific time intervals, the degraded hydrogels were collected and further dried in vacuo. The dry weight of samples after degradation (W_d) was determined and the percentage of weight remaining (%) was calculated as $(W_d/W_i) \times 100$ (Lai & Li, 2010b). Results were the average of four independent measurements.

2.6. Human RPE cell line cultures

ARPE-19 cells, a spontaneously immortalized human cell line (BCRC No. 60383) with morphological and functional characteristics similar to adult human RPE, were purchased from the Bioresource Collection and Research Center (Hsinchu, Taiwan, ROC). The cells were maintained in regular growth medium containing DMEM/F12, 10% FBS, and 1% A/A solution. Cultures were incubated in a humidified atmosphere of 5% CO_2 at 37 °C. The cells from passage 42 were used for experiments.

2.7. In vitro biocompatibility studies

The hydrogel sheets were sterilized in a graded series of ethanol solutions and thoroughly rinsed in sterilized PBS for use in the in vitro experiments. For evaluation of cellular responses to cross-linked HA materials, the method was used as described previously (Lai, Lu, Chen, Tabata, & Hsiue, 2006). In brief, ARPE-19 cells (7×10^4 cells/well) were seeded in 24-well plates and were grown to confluence. Using cell culture inserts (Falcon 3095, Becton Dickinson Labware, Franklin Lakes, NJ, USA), each well of a 24-well plate was divided into two compartments. A test sample ($1\ cm^2 \times 1\ cm^2$ hydrogel sheet) was placed into the inner well of the double-chamber system to examine the cells cultivated on the plastic plate. After a 4-day exposure of cultures to various DVS cross-linked HA materials, the qualitative and quantitative assays were performed following removal of the inserts and test samples. ARPE-19 cells in regular growth medium without hydrogel materials served as control groups (Ctrl).

2.8. Cell viability assays

Cell viability was determined using the Live/Dead Viability/Cytotoxicity Kit from Molecular Probes (Eugene, OR, USA) (Lai, Chen, Hsu, Hsiue, & Lee, 2006). This assay uses intracellular esterase activity to identify the living cells; the process cleaves the calcein acetoxymethyl to produce a green fluorescence. Ethidium homodimer-1 can easily pass through the damaged cell membranes of dead cells to bind to the nucleic acids, yielding a red fluorescence. After washing three times with PBS, the cultures were stained with a working solution consisting of 2 μl of ethidium homodimer-1, 1 ml of PBS, and 0.5 μl of calcein acetoxymethyl. Under fluorescence microscopy (Axiovert 200M; Carl Zeiss, Oberkochen, Germany), three different areas each containing approximately 500 cells were counted at 100× magnification. All experiments were performed in triplicate, and the viability of the ARPE-19 cell cultures was expressed as the average ratio of live cells to the total number of cells in these nine different areas.

2.9. Pro-inflammatory gene and cytokine expression analyses

Total RNA was isolated from cells with TRIzol reagent according to the manufacturer's procedure (Lai et al., 2013). Reverse transcription of the extracted RNA (1 μg) was performed using ImProm-II (Promega, Madison, WI, USA) and Oligo$(dT)_{15}$ primers (Promega). The primers used to amplify the human interleukin-1β (IL-1β) complementary DNA (cDNA) were 5′-AGGATATGGAGCAACAAGTGGT-3′ (sense) and 5′-CGCTTTTCCATCTTCTTCTTTG-3′ (antisense), and those used to amplify the interleukin-6 (IL-6) cDNA were 5′-CCACTCACCTCTTCAGAACGAA-3′ (sense) and 5′-GGCAAGTCTCCTCATTGAATCC-3′ (antisense). The sequences of the primer pair used to amplify the internal control cDNA, glyceraldehyde-3-phosphate dehydrogenase (GAPDH), were 5′-TGGTATCGTGGAAGGACTCATGAC-3′ (sense) and 5′-ATGCCAGTGAGCTTCCCGTTCAGC-3′ (antisense). Quantitative real-time reverse transcription polymerase chain reaction (RT-PCR) was performed on a Light-Cycler instrument (Roche Diagnostics, Indianapolis, IN, USA) according to the manufacturer's instructions with FastStart DNA Master SYBR Green I reagent (Roche Diagnostics). Each sample was determined in triplicate, and the gene expression results were normalized to the level of GAPDH mRNA.

Aliquots of the supernatant were collected to measure the IL-1β and IL-6 levels. The release of IL-1β and IL-6 from cultivated cells into the conditioned medium was detected by the Quantikine enzyme-linked immunosorbent assay (ELISA) kit (R&D Systems, Minneapolis, MN, USA) specific for human IL-1β and IL-6. Cytokine bioassays were performed according to the manufacturer's instructions. Photometric readings at 450 nm were measured using the Multiskan Spectrum Microplate Spectrophotometer (ThermoLabsystems, Vantaa, Finland) (Lai & Li, 2010a). Results were expressed as pg/ml. All experiments were conducted in quadruplicate.

2.10. Glutamate uptake measurements

Before glutamate uptake assays, the cells were washed three times with Krebs-Ringer-Hepes (KRH) buffer (126 mM NaCl, 5.1 mM KCl, 0.81 mM $CaCl_2$, 1.3 mM $MgSO_4$, 1.3 mM NaH_2PO_4, 15 mM Hepes and 10 mM D-glucose, pH 7.4). After exposure of cultures to test materials, the radioactive [^{3}H]glutamate solution, which contained 1.25 μCi [^{3}H]glutamate, and the total glutamate concentration of 5 μM were added to the dishes. Following a further incubation for 10 min, the reaction was terminated by washing three times with ice-cold KRH buffer. The dried cells were dispersed with 0.4 N NaOH and neutralized with HCl. The radioactivity inside the cells was quantitated by using a liquid scintillation counter (Lai, 2009). The results were calculated to the protein content of the cells and expressed as specific activity relative to that of control groups. All experiments were conducted in triplicate.

The protein content of the cells was determined by colorimetric assay using a bicinchoninic acid (BCA) protein assay kit (Pierce Chemical, Rockford, IL, USA) (Ma, Lai, Cheng, Tsai, & Yeh, 2010). The working solution was prepared by mixing a 4% copper (II) sulfate pentahydrate solution with an excess of BCA at a final ratio of 1:50 (v/v); 100 μl of test samples was added to 2 ml of the working reagent. The mixture was incubated at 37 °C for 30 min, and was subsequently cooled to room temperature. The absorbance of the mixture solution was recorded with an UV–vis spectrophotometer (Thermo Scientific, Waltham, MA, USA) at 562 nm using BSA at various known concentrations as standard.

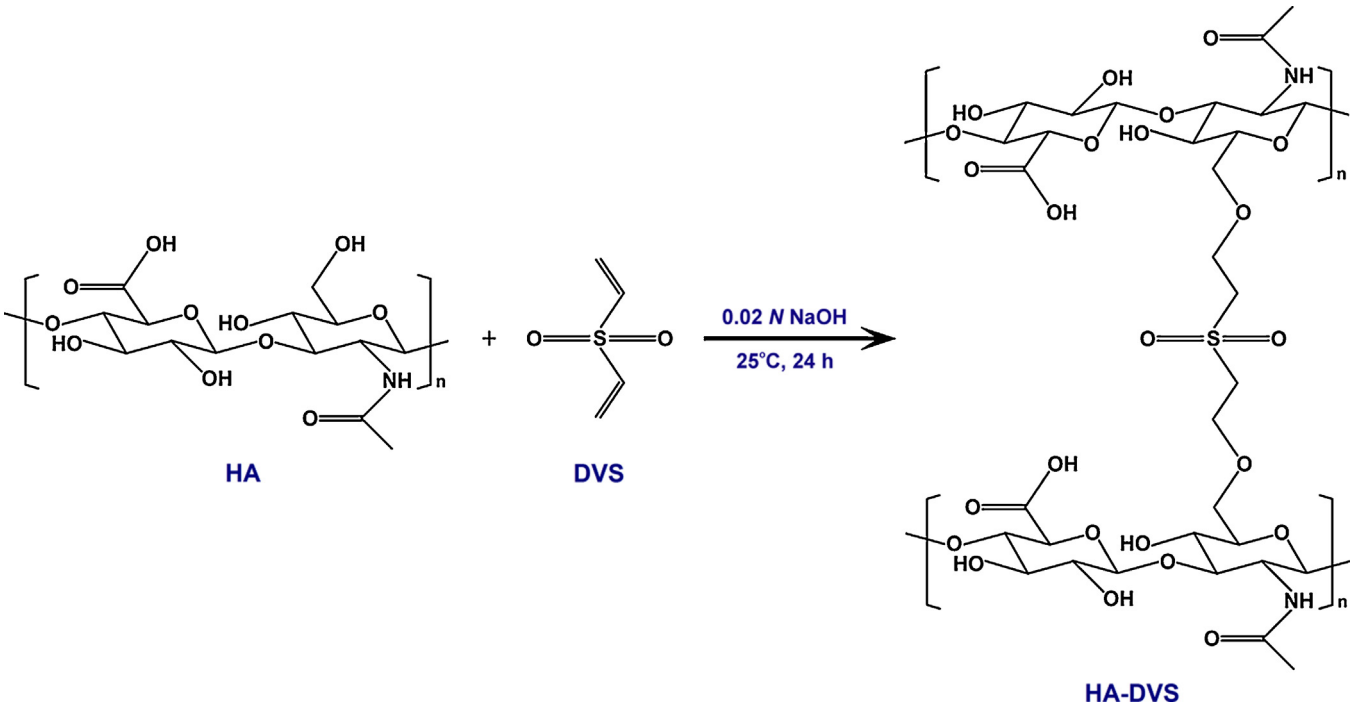

Fig. 1. Cross-linking reaction scheme of HA with DVS.

2.11. Statistical analyses

Results were expressed as mean ± standard deviation (SD). Comparative studies of means were performed using one-way analysis of variance (ANOVA). Significance was accepted with $P < 0.05$.

3. Results and discussion

3.1. Preparation and characterization of DVS cross-linked HA sheets

Cross-linking is an important research issue in biomaterial processing. It may affect the structural strength (Grasman, Page, Dominko, & Pins, 2012), mechanical behavior (Singh, Suri, Tiwary, & Rana, 2012), hydrothermal stability (Burugapalli, Chan, Naik, Kelly, & Pandit, 2009), and degradation profile (Lai, 2011) of modified biomaterials. In particular, the cross-linking reaction dictated by the type and concentration of cross-linker is known to further determine the biocompatibility of test samples. We have previously demonstrated that the carbodiimide treated gelatin hydrogels induce significantly less iris pigment epithelial cellular response compared to its glutaraldehyde cross-linked counterparts (Lai, 2010). A further study has indicated that with the optimum concentration of cross-linking agent, the carbodiimide treated gelatin membranes do not cause any cytotoxicity over 3 days to RPE cells (Lai & Li, 2011). In this work, the chemical cross-linking of HA hydrogel sheets was carried out using DVS. The effect of cross-linker concentration on the safety of modified carbohydrate polymers was investigated by using human RPE cell line cultures. To the best of our knowledge, the relationship between the chemical characterization and cytocompatibility of DVS cross-linked HA sheets has not been documented.

The general reaction mechanism for the DVS cross-linking of HA materials is presented in Fig. 1. Under alkaline conditions, the DVS reacts primarily with the hydroxyl groups of HA to form ether bonds. After chemical treatment, the HA molecules are bridged by DVS (i.e., a non zero-length cross-linker). According to the report by Collins and Birkinshaw (2008a), the reaction of DVS cross-linking is very fast, and this may lead to gel formation within minutes. Fig. 2 shows the results of energy dispersive X-ray spectroscopic analyses for DVS cross-linking of HA hydrogel sheets. The sulfur distribution of various samples was investigated by EDS mapping technique, which has previously been employed to examine the modification of gelatin scaffolds with chondroitin sulfate (Lai, Li, Cho, & Yu, 2012). The images of sample HA-DVS000 showed a homogeneous black area, indicating the absence of sulfur element (Fig. 2a). The observed results are probably due to that HA is a non-sulfated glycosaminoglycan. In contrast, after modification of HA with DVS, the white dots, indicative of detected sulfur element, could be seen on the analyzed image. Additionally, the order of increasing number of white dots for the sheets was HA-DVS100 > HA-DVS050 > HA-DVS025, suggesting that the DVS concentration may play a crucial role in the cross-linking reaction. As shown in Fig. 2b, the EDS spectrograms exhibit the carbon, oxygen, nitrogen, and sodium peaks, which are attributed to the composition of HA. Since the cross-linking agent participated in the formation of covalent bonds, the S signals were detected in all test groups except HA-DVS000 groups. Fig. 2c further shows the sulfur content of chemically modified HA sheets as a function of DVS concentration. The non-cross-linked HA samples from HA-DVS000 groups had no sulfur content. The atomic percentage of sulfur in the HA-DVS025, HA-DVS050, and HA-DVS100 groups was 0.02 ± 0.01%, 0.10 ± 0.03%, and 0.23 ± 0.03%, respectively. There were significant differences among these groups ($P < 0.05$). The results of sulfur content are consistent with qualitative distribution data. Our findings also suggest that an increased concentration of S atom is noted for the HA materials treated with large amount of DVS. The increase in cross-linker concentration may raise the collision frequency and reaction probability between HA and DVS molecules, thereby altering the chemical structure of carbohydrate polymers.

FTIR is a useful tool for the identification of specific molecular structures and interactions in polymers (Lai, Wang, Li, & Tu, 2012). As shown in Fig. 3a, the non-cross-linked samples from HA-DVS000 groups revealed several characteristic bands at

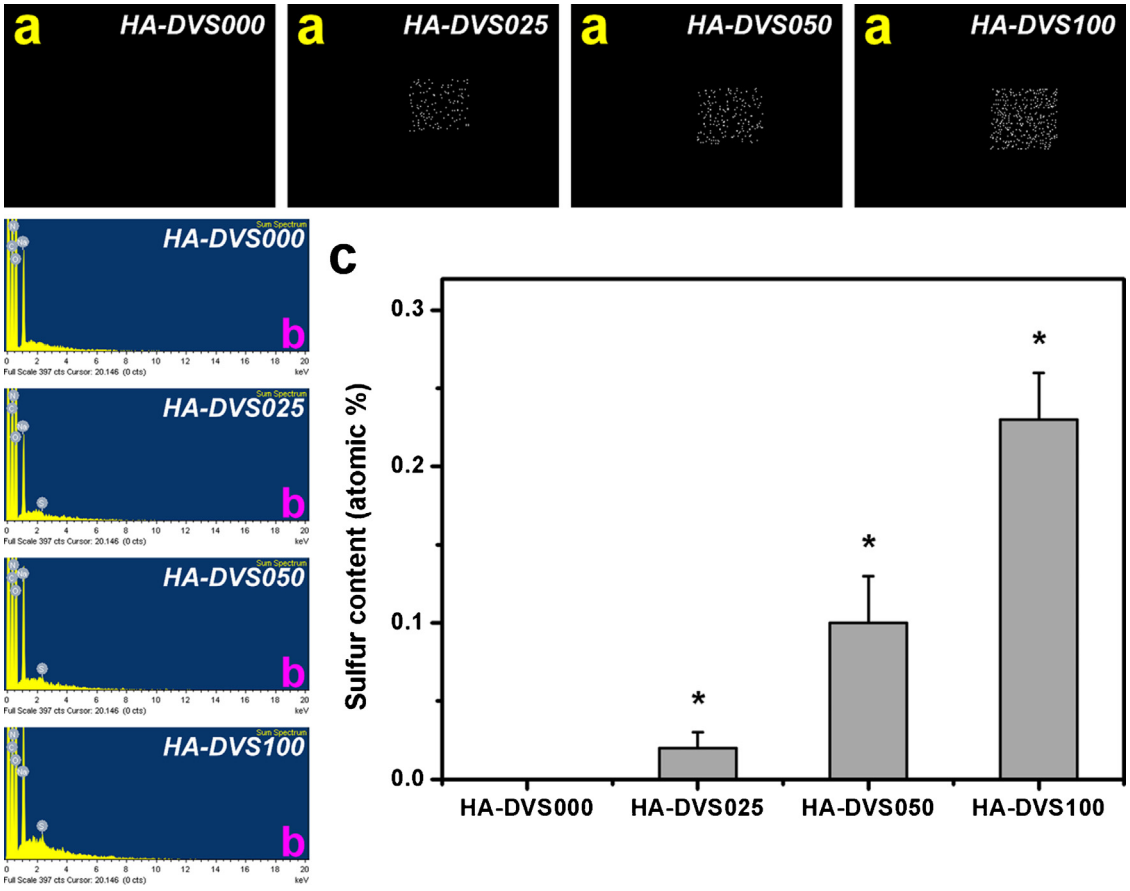

Fig. 2. Energy dispersive X-ray spectroscopy mapping of HA as a function of DVS concentration. (a) EDS mapping of sulfur, (b) EDS spectrogram, and (c) atomic percentage of sulfur. Values are mean ± SD ($n = 3$). *$P < 0.05$ vs all groups.

3265 cm^{-1} (hydrogen-bonded O—H and N—H stretching vibrations), 2885 cm^{-1} (C—H stretching vibrations), 1606 and 1404 cm^{-1} (asymmetric C═O and symmetric C—O stretching modes of the planar carboxyl groups), 1653 (amide I, C═O stretching vibrations), 1548 cm^{-1} (amide II, N—H bending vibrations), 1149 cm^{-1} (C—O—C stretching vibrations), 1028 cm^{-1} (C—OH stretching vibrations). These data are in agreement with previous FTIR study on HA (Wu, 2012). It has also been reported that the spectrum of DVS exhibits absorptions at 1312 cm^{-1} (S═O asymmetric stretching vibrations), 1131 cm^{-1} (S═O symmetric stretching vibrations), 977 cm^{-1} (C—H bending vibrations), and 778 cm^{-1} (S—C stretching vibrations) (Ellzy et al., 2003). In this study, all the DVS cross-linked HA materials had these characteristic peaks. Additionally, after reaction of HA with DVS, the samples showed a small peak at 1261 cm^{-1}, which represents a characteristic stretching frequency of ether bond (Bhattacharyya, Guillot, Dabboue, Tranchant, & Salvetat, 2008). Our data demonstrate that the DVS cross-linking reaction is successful because the sulfonyl-bis-ethyl cross-links are generated between biopolymer chains.

Although a similar pattern of spectra was noted for all the cross-linked HA materials, the peak intensities were dependent on the DVS concentration. The absorption peak ratios are summarized in Fig. 3b. When the concentration of DVS was increased from 25 to 100 mM, the samples showed a significantly decreased ($P < 0.05$) intensity ratio of A_{3265}/A_{1548}, which is indicative of decreased hydroxyl groups following the cross-linking reaction. Meanwhile, a significantly increased ($P < 0.05$) intensity ratio of A_{1261}/A_{1548} was associated with the formation of more ether linkages between the hydroxyl groups of HA. Furthermore, the intensity ratio of A_{1309}/A_{1548} in the HA-DVS025, HA-DVS050, and HA-DVS100 groups was 0.82 ± 0.03, 0.87 ± 0.02, and 0.93 ± 0.03, respectively. There were significant differences among these groups ($P < 0.05$), indicating that the amount of covalently incorporated DVS into the structure of HA may be controlled by the cross-linker concentration. These findings support the EDS measurements (Fig. 2).

3.2. Mechanical tests

Fig. 4 shows the mechanical properties of various DVS cross-linked HA sheets. After placement in an environment with humidity of 75% for 24 h, the non-cross-linked HA samples had a stress at break of about 1 MPa, suggesting poor mechanical stability. This phenomenon is reasonable because HA is a highly hygroscopic molecule (Lai, Ma, et al., 2010). The presence of absorbed water is known to alter the structural strength of hydrophilic biopolymer networks (Lai et al., 2009; Lai, Li, et al., 2012). The stress at break was significantly lower in the HA-DVS025 (8.7 ± 2.1 MPa), compared with those of the HA-DVS050 (13.9 ± 1.6 MPa) and HA-DVS100 (21.3 ± 1.7 MPa) groups ($P < 0.05$) (Fig. 4a). A similar trend was found for the effect of DVS concentration on Young's modulus variation (Fig. 4b). Collins and Birkinshaw (2008b) have previously investigated the mechanical properties of the chemically modified HA gels by uniaxial compression measurements and found that the DVS cross-linked samples are more delicate than their glutaraldehyde treated counterparts. This study further demonstrates that the cross-linker concentration may have a profound influence on mechanical stability of DVS treated HA materials. The same phenomenon is also found in the case of carbodiimide cross-linked

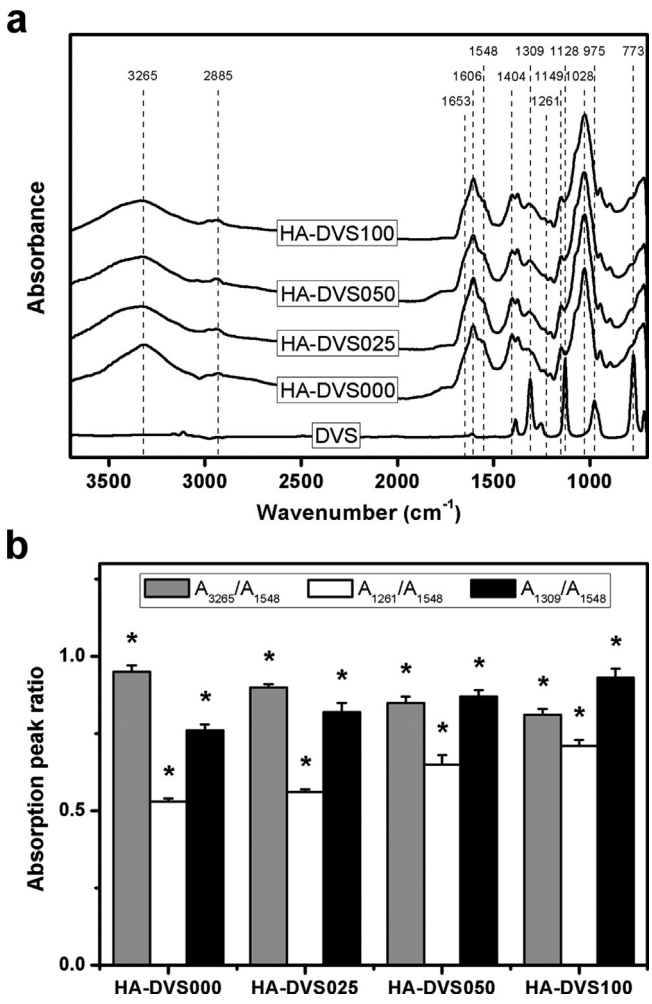

Fig. 3. (a) Fourier transform infrared spectroscopy spectra of DVS and the HA samples cross-linked with varying concentrations of DVS. (b) The absorption peak ratios of the O—H stretching to N—H bending bands (A_{3265}/A_{1548}), C—O stretching to N—H bending bands (A_{1261}/A_{1548}), and S=O stretching to N—H bending bands (A_{1309}/A_{1548}) for the HA samples cross-linked with varying concentrations of DVS. Values are mean ± SD ($n = 3$). *$P < 0.05$ vs all groups (compared only within A_{3265}/A_{1548}, A_{1261}/A_{1548} or A_{1309}/A_{1548} groups).

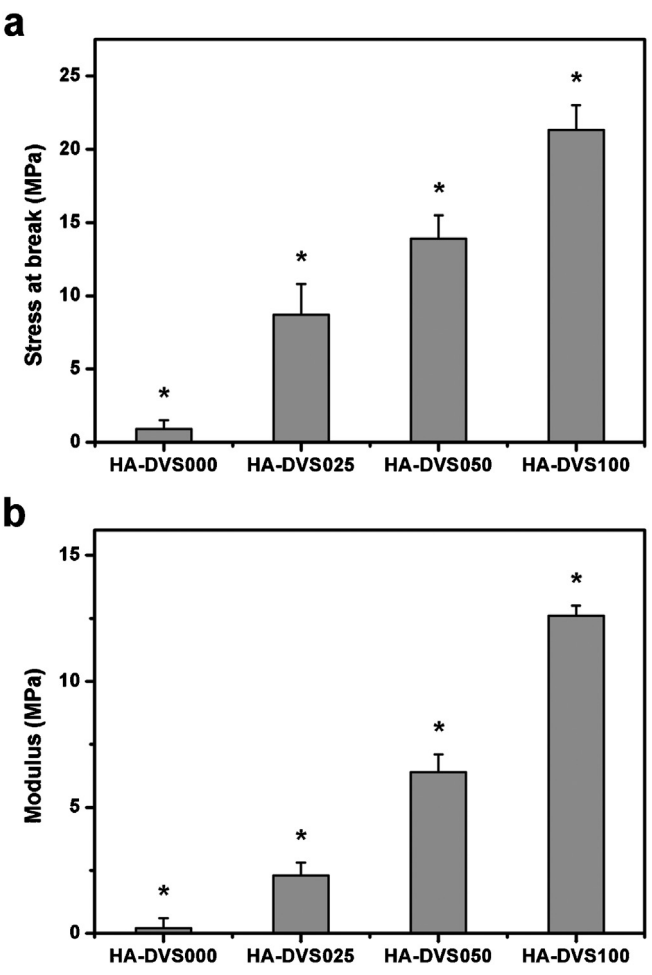

Fig. 4. Mechanical properties of HA samples as a function of DVS concentration. (a) Tensile stress; (b) Young's modulus. Values are mean ± SD ($n = 8$). *$P < 0.05$ vs all groups.

amniotic membrane, which is one of the most commonly used ophthalmic biomaterials for limbal epithelial cell cultivation and transplantation (Ma et al., 2010).

3.3. *In vitro degradation tests*

The resistance against enzymatic degradation of chemically cross-linked HA was determined by immersing the sheets in BSS (i.e., physiological medium) containing hyaluronidase (Lu et al., 2008). Under the action of enzyme, the non-cross-linked HA materials were almost completely degraded within 24 h. Therefore, the residual mass percentage of the DVS treated HA sheets as a function of cross-linker concentration is presented in Fig. 5. After 3 days, the weight remaining in the HA-DVS025, HA-DVS050, and HA-DVS100 groups was 64.6 ± 1.1%, 80.3 ± 2.4%, and 91.5 ± 1.5%, respectively. There were significant differences among these groups ($P < 0.05$). Our recent report has revealed that after 36 h of degradation, the residual mass percentage of HA membranes cross-linked with carbodiimide (100 mM) in the presence of binary acetone/water mixtures containing 85 vol% of acetone is around 65% (Lai, 2012). It may reflect the high cross-linking efficiency of non zero-length

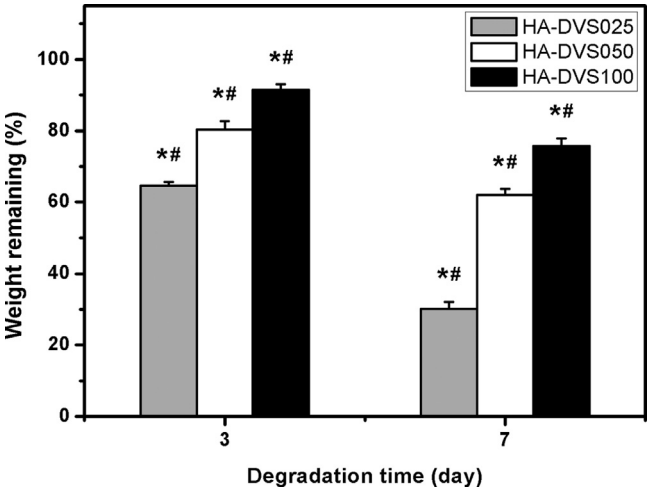

Fig. 5. Weight remaining of various DVS cross-linked HA samples after incubation at 37 °C for 3 and 7 days in BSS containing hyaluronidase. An asterisk indicates statistically significant differences (*$P < 0.05$; $n = 4$) between the 3 and 7 days groups for each type of HA sheet. #$P < 0.05$ vs all groups (compared only within each time point group).

cross-linker such as DVS in the modification of polysaccharide biomaterials. With increasing incubation time from 3 to 7 days, the weight of test samples from each group was significantly decreased ($P < 0.05$). At day 7, a similar trend was found for the effect of cross-linker concentration on weight remaining variation. Our data also suggest that the slower degradation rate of the HA sheets possibly results from the limited access of enzyme to the active sites of the biopolymer chains by the presence of large amount of covalently incorporated DVS. More recently, investigators have shown that the solution properties of HA during the dissolution process are critical to affect the cross-linking efficiency and degradation time of carbodiimide cross-linked HA films (Collins & Birkinshaw, 2013b). In this study, the material stability against enzymatic cleavage is highly correlated with the molecular structure of chemically modified carbohydrate polymers.

3.4. Cell viability assays

A recent review paper by Collins and Birkinshaw (2013a) has summarized the researches on the modification and cross-linking of HA used in tissue engineering. The prerequisite is that the chemically treated biopolymers must be non-toxic toward the cells. Here, the cytocompatibility of the DVS cross-linked HA hydrogel sheet was investigated by means of Live/Dead assays. Fig. 6a shows representative fluorescent images of human RPE cultures, where the live cells fluoresce green and the dead ones fluoresce red. After a 4-day exposure of ARPE-19 cultures to various test materials, prominent green fluorescence was found for the Ctrl, HA-DVS000, HA-DVS025, and HA-DVS050 groups. Additionally, the cells had only a few red-stained nuclei, indicating no cytotoxicity of these samples. In contrast, the cultures from the HA-DVS100 groups contained a large number of dead cells, implying that the HA treated with the highest concentration of DVS (100 mM) may cause noticeable cytotoxicity.

Fig. 6b further shows the results of quantitative analysis of cell viability. In the Ctrl groups, the mean percentage of live cells was $99.0 \pm 0.8\%$, which represents a relatively high viability level of normal RPE cultures. After a 4-day exposure of ARPE-19 cells to test materials, the mean percentage of live cells in the HA-DVS000, HA-DVS025, and HA-DVS050 groups was $98.7 \pm 0.8\%$, $97.9 \pm 1.0\%$, and $97.4 \pm 1.1\%$, respectively. These values did not show a statistically significant difference ($P > 0.05$). The present data also demonstrate that the majority of cultures are viable in the presence of HA sheets treated with concentrations of DVS ranging from 0 to 50 mM. However, the mean percentage of live cells was $85.2 \pm 1.9\%$, which was significantly lower than those of all the other groups ($P < 0.05$). These findings suggest that the cross-linker concentration for the reaction of HA and DVS may affect the cell viability. As reported in the literature, the cross-linked HA gels containing a low concentration of DVS-HA are able to retain the biological characteristics of uncross-linked HA, indicating that the DVS-HA does not compromise the biocompatibility of HA molecules (Ibrahim et al., 2010). Our results are in accordance with this observation. On the other hand, it is noteworthy that when the DVS concentration reached 100 mM, the chemically modified polysaccharide biomaterials are not well tolerated during 4 days of RPE cell culture. Yeom et al. (2010) have pointed out that the possible toxic remaining groups of DVS in HA-DVS hydrogels cannot be excluded. Recently, West, Stamm, Brown, Justice, and Morano (2011) have demonstrated that the bifunctional electrophile DVS may be detrimental to cellular homeostasis and cause cytotoxicity in colorectal carcinoma cells. These findings may account for a 15% reduction in RPE cell viability due to exposure to the HA cross-linked with the highest DVS concentration in this study.

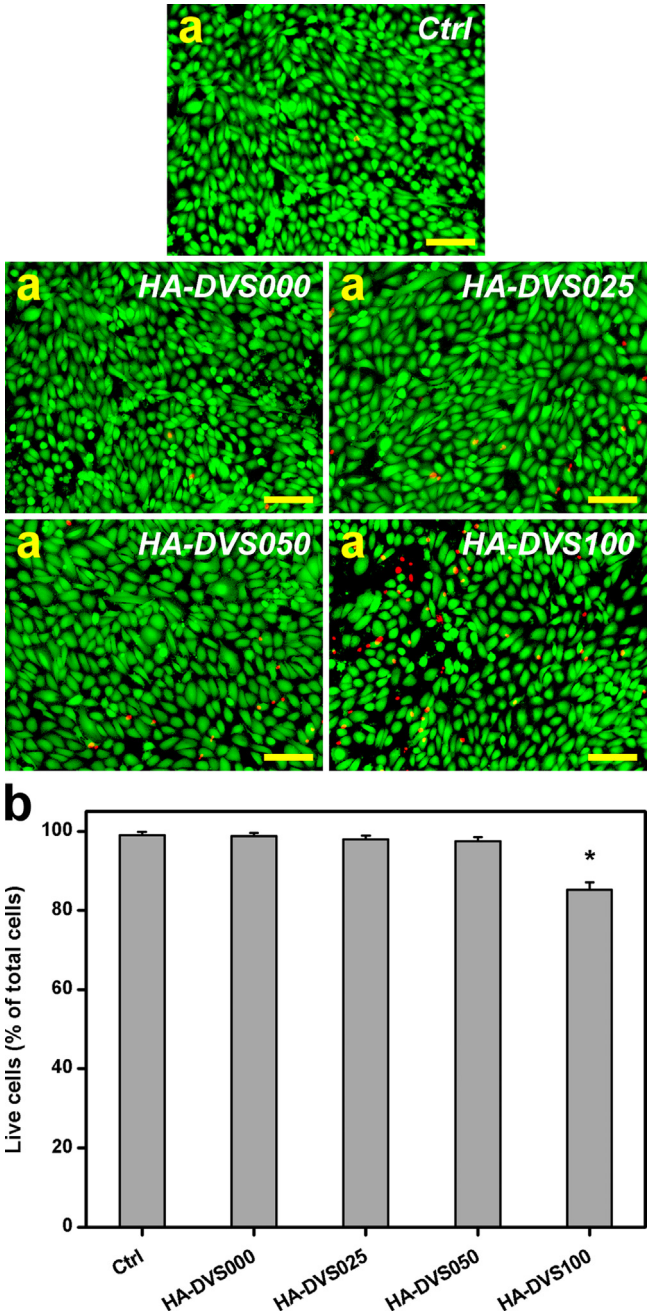

Fig. 6. (a) Cell viability of ARPE-19 cultures was determined by staining with Live/Dead Viability/Cytotoxicity Kit in which live cells fluoresce green and dead cells fluoresce red. Fluorescence images of cells after exposure to various DVS cross-linked HA materials for 4 days at 37 °C. Ctrl: without materials. Scale bars: 50 μm. (b) Mean percentage of live cells in the ARPE-19 cultures exposed to various DVS cross-linked HA materials as measured by the Live/Dead assay. An asterisk indicates statistically significant differences (*$P < 0.05$; $n = 9$) as compared to the Ctrl groups.

3.5. Pro-inflammatory gene and cytokine expression analyses

It has been documented that pro-inflammatory IL-1β and IL-6 expressions associated with the local reaction of retinal tissues are detected after the early days of transplantation of human RPE cells into the subretinal space (Abe et al., 1999). The transcription of IL-1β and IL-6 genes was therefore evaluated by quantitative real-time RT-PCR. After a 4-day exposure of ARPE-19 cultures to various test materials, the results of gene expression levels normalized to GAPDH are shown in Fig. 7a. The transcript level in the Ctrl groups for each gene was set to 100% here. In the HA-DVS000 groups, the

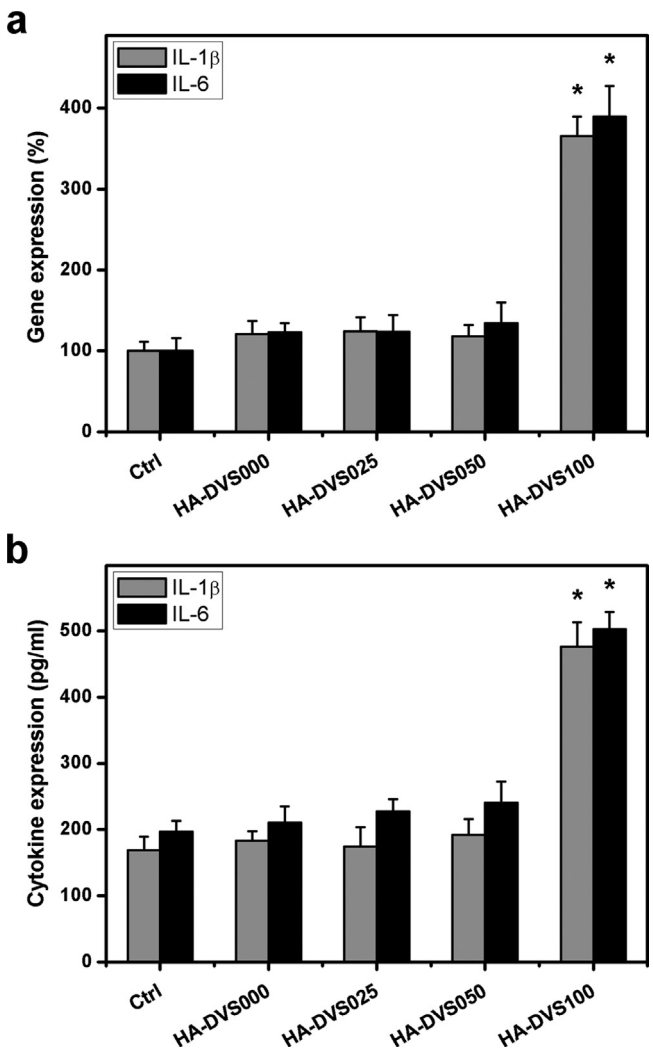

Fig. 7. (a) Gene expression of IL-1β and IL-6 in ARPE-19 cells incubated with various DVS cross-linked HA materials for 4 days. Normalization was done by using GAPDH. Data in the experimental groups are percentages relative to that of Ctrl groups (without materials). An asterisk indicates statistically significant differences ($^*P < 0.05$; $n = 3$) versus Ctrl (compared only within IL-1β or IL-6 groups). (b) Level of IL-1β and IL-6 released from ARPE-19 cultures after exposure to various DVS cross-linked HA materials for 4 days. The cultures in absence of HA materials serve as Ctrl groups. An asterisk indicates statistically significant differences ($^*P < 0.05$; $n = 4$) versus Ctrl (compared only within IL-1β or IL-6 groups).

IL-1β mRNA expression was 120.7 ± 16.5%, which was not significantly different compared with HA-DVS025 (124.4 ± 17.1%) and HA-DVS050 (118.0 ± 13.8%) groups ($P > 0.05$), but was significantly lower than that of the HA-DVS100 (365.6 ± 24.0%) groups ($P < 0.05$). In addition, the IL-6 gene expression of the HA-DVS000, HA-DVS025, and HA-DVS050 groups was 123.1 ± 11.0%, 123.6 ± 20.8%, and 134.2 ± 25.5%, respectively. A significant up-regulation of IL-6 mRNA expression was found in the HA-DVS100 groups compared with the other groups ($P < 0.05$), indicating that this hydrogel sample promotes inflammation.

Fig. 7b further shows the ARPE-19 cell secretion of IL-1β and IL-6 in response to various test materials. The measured concentration of IL-1β in the HA-DVS100 groups was 476.5 ± 36.2 pg/ml, which was significantly higher than those in the Ctrl (168.6 ± 20.5 pg/ml), HA-DVS000 (183.0 ± 14.2 pg/ml), HA-DVS025 (174.1 ± 29.3 pg/ml), and HA-DVS050 (192.2 ± 24.0 pg/ml) groups ($P < 0.05$). There was no statistically significant difference in the IL-6 level between the Ctrl and experimental groups treated with cross-linker concentrations ranging from 0 to 50 mM ($P > 0.05$). By contrast, significantly higher concentrations of IL-6 were noted after incubation with samples cross-linked with 100 mM DVS ($P < 0.05$). Our results indicate that the IL-1β and IL-6 cytokine production levels of human RPE cell cultures exposed to various HA materials follow the same trend as their respective pro-inflammatory gene expressions. The amount of covalently incorporated DVS into the structure of HA may have an important role in the stimulation of pro-inflammatory cytokine production in human RPE cells.

Ocular biocompatibility of HA hydrogels has previously been investigated by us using the anterior chamber of a rabbit eye model (Lai, Ma, et al., 2010). The residence of non-cross-linked HA implants in the intraocular cavity does not elicit tissue response and adverse inflammatory reaction. Oh et al. (2008) have also demonstrated that there is no inflammation at the injection sites of the rabbits receiving HA solution. Interestingly, their HA-DVS hydrogel sample appears to be biocompatible, based on the histological examination. However, the group of Ramamurthi has further found that the use of high concentrations of DVS is necessary to fabricate solid gels, but the cross-linking agent may compromise the biocompatibility of polysaccharide biomaterials (Ibrahim et al., 2010). Although its toxicity mechanism remains unclear, DVS has been reported to be able to selectively inactivate GAPDH, which is one of glycolytic enzymes responsible for the cell damage (Sok, Choi, Kim, Lee, & Cha, 1993). Theoretically, the chemical cross-linker is supposed to modulate cell function at the molecular level. For the first time, the findings of this study suggest that the HA hydrogels treated with the highest DVS concentration adversely affect the RPE cells and elevate pro-inflammatory genes and cytokines.

3.6. Glutamate uptake measurements

RPE is a monolayer of cuboidal cells located between the choriocapillaris and the neural retina, and these cells mediate the transport of metabolic intermediates, waste products, ions and fluid components (Lai & Li, 2011). Another crucial function of the RPE is to maintain the concentration of glutamate, which is the main excitatory neurotransmitter in the retina. It has been reported that the glutamate concentration in the subretinal space regulated by glutamate uptake in the RPE cells is highly correlated with a Na^+-dependent active transport system (Miyamoto & Del Monte, 1994). In this work, the glutamate uptake assays were therefore performed on ARPE-19 cells exposed to the DVS cross-linked HA hydrogel sheets. After incubation with various test materials for 4 days, the RPE cell cultures were analyzed for their glutamate uptake capacity. As shown in Fig. 8, the glutamate uptake activity in the HA-DVS000, HA-DVS025, and HA-DVS050 groups was 93.1 ± 4.0%, 92.7 ± 5.2%, and 89.8 ± 6.6%, respectively. These values did not reveal a statistically significant difference ($P > 0.05$). However, the activity level was 76.5 ± 4.3%, which was significantly lower than those of all the other groups ($P < 0.05$). Results of this study suggest that the cross-linker concentration for the reaction of HA and DVS may affect the glutamate uptake capacity of the cells. We have investigated the effect of Bloom index of gelatin on the regulation of glutamate uptake and found that the high-Bloom-strength gelatins with high viscosity reduce the nutrient availability to cultured ARPE-19 cells and decrease the uptake activity (Lai, 2009). It is known that intermolecular cross-linking between different polymer chains leads to an increase in viscosity and finally to a gelation of the system (Gebben, van den Berg, Bargeman, & Smolders, 1985). This may account for when the DVS concentration reaches 100 mM, the chemically modified HA with the highest extent of cross-linking causes reduction in glutamate uptake by human RPE cells.

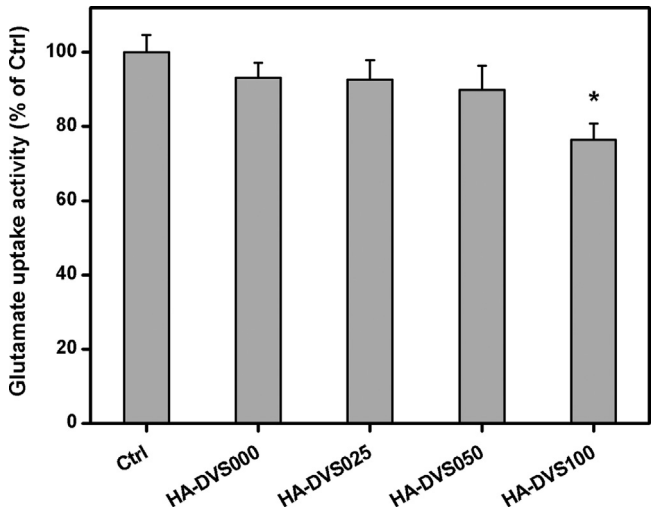

Fig. 8. Glutamate uptake in the ARPE-19 cultures after exposure to various DVS cross-linked HA materials for 4 days. Data in the experimental groups are percentages relative to that of Ctrl groups (without materials). An asterisk indicates statistically significant differences ($^*P < 0.05$; $n = 3$) as compared to the Ctrl groups.

4. Conclusions

Biocompatibility is one of the most important prerequisites in the development of biomaterial technologies. This paper investigates the effect of molecular structure of DVS cross-linked HA on its cytocompatibility. Results of chemical characterization studies showed that the amount of covalently incorporated DVS into the structure of HA is largely controlled by the cross-linker concentration, thereby determining the mechanical stability and resistance against enzymatic degradation. Using cell viability assays, pro-inflammatory gene and cytokine expression analyses, and glutamate uptake measurements, we found that the RPE cellular responses to the chemically modified carbohydrate polymers also depend on the cross-linking condition for the reaction of HA and DVS. The present study demonstrates good cytocompatibility of HA sheets treated with concentrations of DVS ranging from 0 to 50 mM. The understanding of cell-material interactions may gain further insight into the design and optimization of biocompatible DVS cross-linked HA hydrogels for potential use in the delivery of cell and drug therapeutics to treat posterior segment diseases.

Acknowledgements

This work was supported by Grant NSC102-2628-B-182-017-MY3 from the National Science Council of Republic of China and Grant CMRPD2A0111 from Chang Gung Memorial Hospital. The author is grateful to Ya-Ting Li (Institute of Biochemical and Biomedical Engineering, Chang Gung University) for technical assistance.

References

Abe, T., Takeda, Y., Yamada, K., Akaishi, K., Tomita, H., Sato, M., et al. (1999). Cytokine gene expression after subretinal transplantation. *Tohoku Journal of Experimental Medicine*, *189*(3), 179–189.

Bhattacharyya, S., Guillot, S., Dabboue, H., Tranchant, J. F., & Salvetat, J. P. (2008). Carbon nanotubes as structural nanofibers for hyaluronic acid hydrogel scaffolds. *Biomacromolecules*, *9*(2), 505–509.

Burugapalli, K., Chan, J. C. Y., Naik, H., Kelly, J. L., & Pandit, A. (2009). Tailoring the properties of cholecyst-derived extracellular matrix using carbodiimide cross-linking. *Journal of Biomaterials Science, Polymer Edition*, *20*(7–8), 1049–1063.

Collins, M. N., & Birkinshaw, C. (2008a). Investigation of the swelling behavior of crosslinked hyaluronic acid films and hydrogels produced using homogeneous reactions. *Journal of Applied Polymer Science*, *109*(2), 923–931.

Collins, M. N., & Birkinshaw, C. (2008b). Physical properties of crosslinked hyaluronic acid hydrogels. *Journal of Materials Science Materials in Medicine*, *19*(11), 3335–3343.

Collins, M. N., & Birkinshaw, C. (2013a). Hyaluronic acid based scaffolds for tissue engineering – A review. *Carbohydrate Polymers*, *92*(2), 1262–1279.

Collins, M. N., & Birkinshaw, C. (2013b). Hyaluronic acid solutions – A processing method for efficient chemical modification. *Journal of Applied Polymer Science*, *130*(1), 145–152.

Ellzy, M. W., Jensen, J. O., & Kay, J. G. (2003). Vibrational frequencies and structural determinations of di-vinyl sulfone. *Spectrochimica Acta Part A – Molecular and Biomolecular Spectroscopy*, *59*(4), 867–881.

Fine, S. L., Berger, J. W., Maguire, M. G., & Ho, A. C. (2000). Age-related macular degeneration. *New England Journal of Medicine*, *342*(7), 483–492.

Gebben, B., van den Berg, H. W. A., Bargeman, D., & Smolders, C. A. (1985). Intramolecular crosslinking of poly(vinyl alcohol). *Polymer*, *26*(11), 1737–1740.

Grasman, J. M., Page, R. L., Dominko, T., & Pins, G. D. (2012). Crosslinking strategies facilitate tunable structural properties of fibrin microthreads. *Acta Biomaterialia*, *8*(11), 4020–4030.

Hahn, S. K., Jelacic, S., Maier, R. V., Stayton, P. S., & Hoffman, A. S. (2004). Anti-inflammatory drug delivery from hyaluronic acid hydrogels. *Journal of Biomaterials Science, Polymer Edition*, *15*(9), 1111–1119.

Ibrahim, S., Kang, Q. K., & Ramamurthi, A. (2010). The impact of hyaluronic acid oligomer content on physical, mechanical, and biologic properties of divinyl sulfone-crosslinked hyaluronic acid hydrogels. *Journal of Biomedical Materials Research Part A*, *94A*(2), 355–370.

Jeng, B. H., Hoyt, C. S., & McLeod, S. D. (2004). Completion rate of continuous curvilinear capsulorhexis in pediatric cataract surgery using different viscoelastic materials. *Journal of Cataract and Refractive Surgery*, *30*(1), 85–88.

Lai, J.-Y. (2009). The role of Bloom index of gelatin on the interaction with retinal pigment epithelial cells. *International Journal of Molecular Sciences*, *10*(8), 3442–3456.

Lai, J.-Y. (2010). Biocompatibility of chemically cross-linked gelatin hydrogels for ophthalmic use. *Journal of Materials Science Materials in Medicine*, *21*(6), 1899–1911.

Lai, J.-Y. (2011). Evaluation of cross-linking time for porous gelatin hydrogels on cell sheet delivery performance. *Journal of Mechanics in Medicine and Biology*, *11*(5), 967–981.

Lai, J.-Y. (2012). Solvent composition is critical for carbodiimide cross-linking of hyaluronic acid as an ophthalmic biomaterial. *Materials*, *5*(10), 1986–2002.

Lai, J.-Y., Chen, K.-H., Hsu, W.-M., Hsiue, G.-H., & Lee, Y.-H. (2006). Bioengineered human corneal endothelium for transplantation. *Archives of Ophthalmology*, *124*(10), 1441–1448.

Lai, J.-Y., Chen, K.-H., Hsu, W.-M., Lee, T.-H., & Lin, S.-Y. (2005). Multiple elements in the deposits of opacified Hydroview intraocular lens. *American Journal of Ophthalmology*, *139*(6), 1123–1125.

Lai, J.-Y., & Hsieh, A.-C. (2012). A gelatin-*g*-poly(*N*-isopropylacrylamide) biodegradable in situ gelling delivery system for the intracameral administration of pilocarpine. *Biomaterials*, *33*(7), 2372–2387.

Lai, J.-Y., & Li, Y.-T. (2010a). Evaluation of cross-linked gelatin membranes as delivery carriers for retinal sheets. *Materials Science and Engineering C*, *30*(5), 677–685.

Lai, J.-Y., & Li, Y.-T. (2010b). Functional assessment of cross-linked porous gelatin hydrogels for bioengineered cell sheet carriers. *Biomacromolecules*, *11*(5), 1387–1397.

Lai, J.-Y., & Li, Y.-T. (2011). Influence of cross-linker concentration on the functionality of carbodiimide cross-linked gelatin membranes for retinal sheet carriers. *Journal of Biomaterials Science, Polymer Edition*, *22*(1–3), 277–295.

Lai, J.-Y., Li, Y.-T., Cho, C.-H., & Yu, T.-C. (2012). Nanoscale modification of porous gelatin scaffolds with chondroitin sulfate for corneal stromal tissue engineering. *International Journal of Nanomedicine*, *7*, 1101–1114.

Lai, J.-Y., Li, Y.-T., & Wang, T.-P. (2010). In vitro response of retinal pigment epithelial cells exposed to chitosan materials prepared with different cross-linkers. *International Journal of Molecular Sciences*, *11*(12), 5256–5272.

Lai, J.-Y., Lin, P.-K., Hsiue, G.-H., Cheng, H.-Y., Huang, S.-J., & Li, Y.-T. (2009). Low Bloom strength gelatin as a carrier for potential use in retinal sheet encapsulation and transplantation. *Biomacromolecules*, *10*(2), 310–319.

Lai, J.-Y., Lu, P.-L., Chen, K.-H., Tabata, Y., & Hsiue, G.-H. (2006). Effect of charge and molecular weight on the functionality of gelatin carriers for corneal endothelial cell therapy. *Biomacromolecules*, *7*(6), 1836–1844.

Lai, J.-Y., Ma, D. H.-K., Cheng, H.-Y., Sun, C.-C., Huang, S. J., Li, Y.-T., et al. (2010). Ocular biocompatibility of carbodiimide cross-linked hyaluronic acid hydrogels for cell sheet delivery carriers. *Journal of Biomaterials Science, Polymer Edition*, *21*(3), 359–376.

Lai, J.-Y., Ma, D. H.-K., Lai, M.-H., Li, Y.-T., Chang, R.-J., & Chen, L.-M. (2013). Characterization of cross-linked porous gelatin carriers and their interaction with corneal endothelium: Biopolymer concentration effect. *PLoS One*, *8*(1), e54058.

Lai, J.-Y., & Tu, I.-H. (2012). Adhesion, phenotypic expression, and biosynthetic capacity of corneal keratocytes on surfaces coated with hyaluronic acid of different molecular weights. *Acta Biomaterialia*, *8*(3), 1068–1079.

Lai, J.-Y., Wang, T.-P., Li, Y.-T., & Tu, I.-H. (2012). Synthesis, characterization and ocular biocompatibility of potential keratoprosthetic hydrogels based on photopolymerized poly(2-hydroxyethyl methacrylate)-*co*-poly(acrylic acid). *Journal of Materials Chemistry*, *22*(5), 1812–1823.

Lu, P.-L., Lai, J.-Y., Ma, D. H.-K., & Hsiue, G.-H. (2008). Carbodiimide cross-linked hyaluronic acid hydrogels as cell sheet delivery vehicles: Characterization and interaction with corneal endothelial cells. *Journal of Biomaterials Science, Polymer Edition*, *19*(1), 1–18.

Ma, D. H.-K., Lai, J.-Y., Cheng, H.-Y., Tsai, C.-C., & Yeh, L.-K. (2010). Carbodiimide cross-linked amniotic membranes for cultivation of limbal epithelial cells. *Biomaterials*, *31*(25), 6647–6658.

McDonald, C. C., Kaye, S. B., Figueiredo, F. C., Macintosh, G., & Lockett, C. (2002). A randomised, crossover, multicentre study to compare the performance of 0.1% (w/v) sodium hyaluronate with 1.4% (w/v) polyvinyl alcohol in the alleviation of symptoms associated with dry eye syndrome. *Eye*, *16*(5), 601–607.

Miyamoto, Y., & Del Monte, M. A. (1994). Na^+-dependent glutamate transporter in human retinal pigment epithelial cells. *Investigative Ophthalmology & Visual Science*, *35*(10), 3589–3598.

Murata, M., & Horiuchi, S. (2005). Hyaluronan synthases, hyaluronan and its CD44 receptors in the posterior segment of rabbit eye. *Ophthalmologica*, *219*(5), 287–291.

Oh, E. J., Kang, S. W., Kim, B. S., Jiang, G., Cho, I. H., & Hahn, S. K. (2008). Control of the molecular degradation of hyaluronic acid hydrogels for tissue augmentation. *Journal of Biomedical Materials Research Part A*, *86A*(3), 685–693.

Sannino, A., Madaghiele, M., Conversano, F., Mele, G., Maffezzoli, A., Netti, P. A., et al. (2004). Cellulose derivative-hyaluronic acid-based microporous hydrogels cross-linked through divinyl sulfone (DVS) to modulate equilibrium sorption capacity and network stability. *Biomacromolecules*, *5*(1), 92–96.

Singh, K., Suri, R., Tiwary, A. K., & Rana, V. (2012). Chitosan films: Crosslinking with EDTA modifies physicochemical and mechanical properties. *Journal of Materials Science Materials in Medicine*, *23*(3), 687–695.

Sok, D. E., Choi, D. S., Kim, Y. B., Lee, Y. H., & Cha, S. H. (1993). Selective inactivation of glyceraldehyde-3-phosphate dehydrogenase by vinyl sulfones. *Biochemical and Biophysical Research Communications*, *195*(3), 1224–1229.

West, J. D., Stamm, C. E., Brown, H. A., Justice, S. L., & Morano, K. A. (2011). Enhanced toxicity of the protein cross-linkers divinyl sulfone and diethyl acetylenedicarboxylate in comparison to related monofunctional electrophiles. *Chemical Research in Toxicology*, *24*(9), 1457–1459.

Wu, Y. (2012). Preparation of low-molecular-weight hyaluronic acid by ozone treatment. *Carbohydrate Polymers*, *89*(2), 709–712.

Yeom, J., Bhang, S. H., Kim, B. S., Seo, M. S., Hwang, E. J., Cho, I. H., et al. (2010). Effect of cross-linking reagents for hyaluronic acid hydrogel dermal fillers on tissue augmentation and regeneration. *Bioconjugate Chemistry*, *21*(2), 240–247.

Zhao, X. (2006). Synthesis and characterization of a novel hyaluronic acid hydrogel. *Journal of Biomaterials Science, Polymer Edition*, *17*(4), 419–433.